3 Reaction Kinetics for 1-Hexene Dimerisation

3.1 Background

A kinetic model poses a simplistic means of optimising a preferred reaction to the desired product without the need of excessive experiments. A good kinetic model simplifies and encapsulates the important steps in the reaction mechanism. Literature is however limited on the reaction kinetics over SPA. The work has focused mainly on examining the product spread at a constant space velocity (Ipatieff, 1938; De Klerk, 2004; De Klerk *et al.*, 2004) rather than focusing on trend differences when a single parameter is varied.

Where the reaction rate has been measured over SPA grouping of components is inevitably assumed, especially for components of identical length (Paynter & Schuette, 1971; McClean, 1987; Coa *et al.* 1988). It has been shown for butene oligomerisation, that the reactivity of the olefins is connected to the position of the double bond as well as the degree of branching. Even though isomerisation is known to occur over SPA, the rate of isomerisation (both double bond and skeletal isomerisation) has been ignored during the modelling of the reaction rate (McClean, 1987). Paynter & Schuette (1971) did accommodate for the difference in the reactivity observed fro 1-butene and 2-butene but no allowances was made for the differences in the reactivity of iso-butene. Coa *et al.* (1988) incorporated isomerisation but only in modelling the formation of a non-reactive isomer, which could easily have been a pseudo equilibrium. If the feed isomer composition is not varied, lumping these isomers together would not alter the modelling of the reaction rate. Large differences in the reactivity of isomers have been measured in the literature, suggesting the need for the addition of extra parameters in modelling the rate description.

Since little is known about the dimerisation of 1-hexene over SPA, 1-hexene can be used as a model light naphtha feed for the production of distillate (diesel and jet fuel). Measuring the reaction progression will give insight into the reaction over SPA in terms of *1)* the formation of hexene isomers and the dimerised product, as well as *2)* the effect of temperature on the product spectrum, especially with regard to cracking and secondary dimerisation. To decouple the rate of dimerisation for linear and branched hexenes (and their respective isomers), in this investigation the reaction rate for the dimerisation of 1-hexene and 2,3-dimethyl-1-butene (DMB) was measured in a batch reactor from 100 to 250 °C at 6 MPa.

3.2 Experimental

3.2.1 Materials

The SPA catalyst used during this investigation was obtained from Süd-Chemie Sasolburg (properties listed in Table 3-1). Due to the hydrophilic nature of the catalyst, the catalyst was dried at 200 ^{o}C overnight before each run.

Table 3-1: SPA C84/3 Properties

Free acid (%)	25
Total acid (%)	76
Ortho:pyro silicon phosphates ratio	2.2:1
Pore volume ($cm^3.g^{-1}$)	0.12
Main metal impurities	
Fe (mass %)	0.4
Al (mass %)	0.1

The dimerisation of hexenes was completed with two different hexene isomers, namely 1-hexene (97%) and 2,3-dimethyl-2-butene (DMB) (98%). Tetradecane (99%) was used as solvent to ensure that the reaction remained in the liquid phase. All the chemicals were supplied by Sigma-Aldrich.

3.2.2 Experimental setup and method

All the experiments were conducted in a 200-ml stainless steel batch reactor setup, illustrated in Figure 3-1.

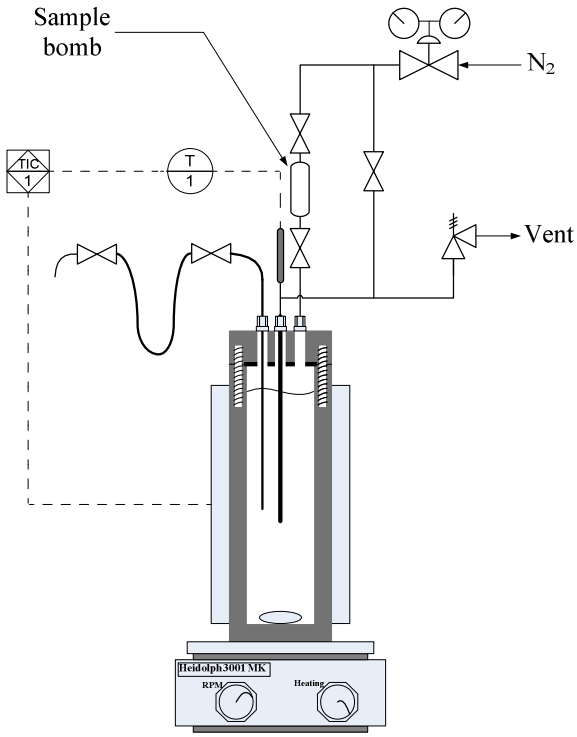

Figure 3-1: Experimental setup

The reactor pressure was controlled by a pressure regulator using a N_2 blanket. Approximately 5 g of the milled catalyst was loaded in the reactor vessel together with 75 g of solvent. This solvent/catalyst mixture was then heated to the desired reaction temperature at a pressure of 1 MPa. Once the required temperature had been reached, 35 g of the chosen hexene isomer was charged to the reactor from a sample bomb by increasing the pressure to 6 MPa – where it was maintained for the remainder of the reaction. This was taken as the start of the reaction and a sample was taken at this point to determine the exact composition of the initial mixture. Although a slight drop in temperature (less than 5% of the set point temperature, meaning if the set point temperature was 200 °C the temperature drop was to 190 °C) was observed after the addition of the hexene reactant, the temperature was re-established before the next sample was taken, where it was controlled within 1 °C of the desired set point, using a heating jacket fitted with a temperature controller. The reaction mixture was agitated with a Heidolph 3001 MK magnetic stirrer at a rate of 1000 rpm after establishing that this would be sufficient to eliminate any external mass transfer effects (Figure 3-2). A further experiment was done whereby the catalyst was milled to 150 µm and 300 µm to determine if internal mass transfer was limiting (Figure 3-3).

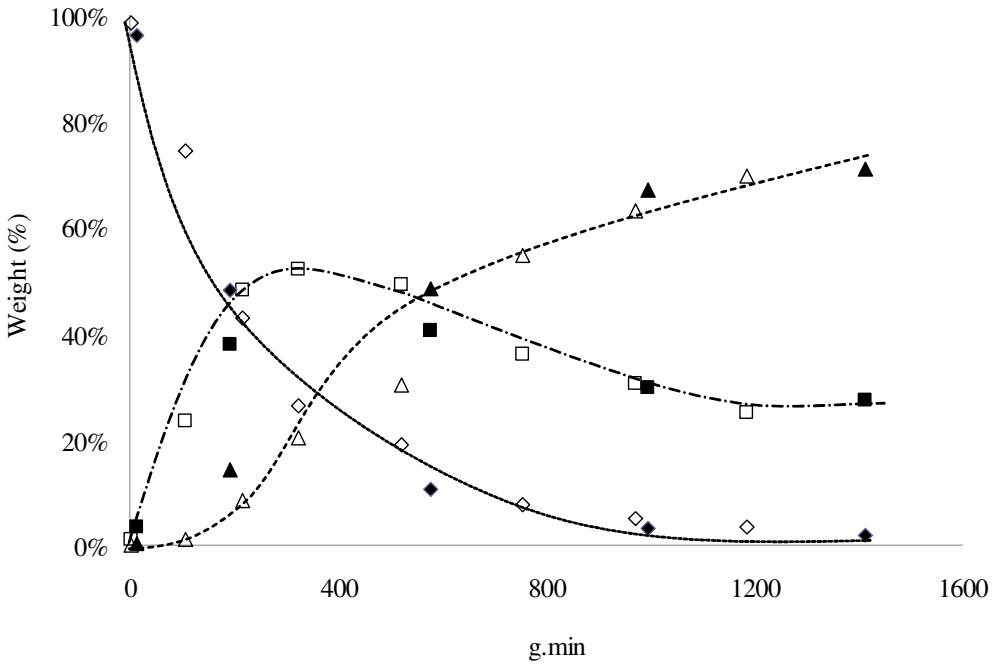

Figure 3-2: 1-Hexene reaction progression at 250 °C versus weight time (g_{cat}.min). Weight fraction of: ◊ = Linear hexene isomers; □ = skeletal hexene isomers and △ = overall hexene depletion (D). The stirrer speed is indicated by the open (500 rpm) and solid (1000 rpm) data points.

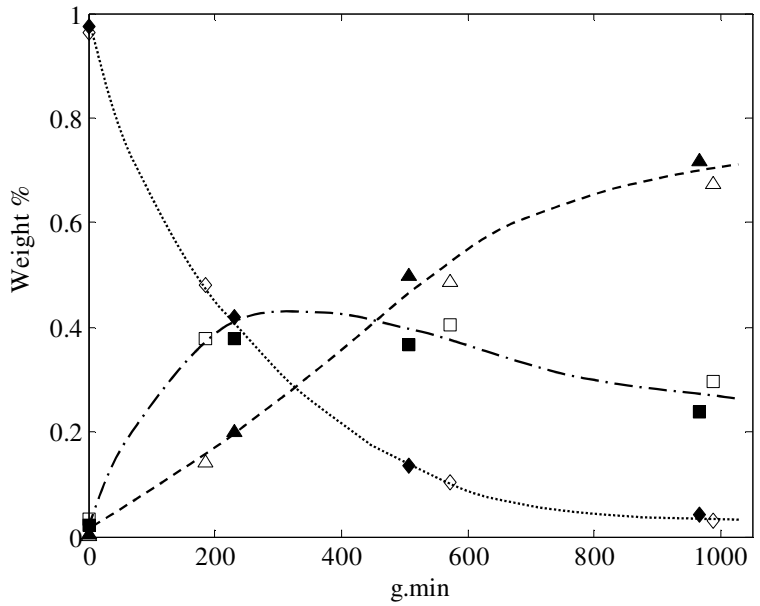

Figure 3-3: The reaction rate of 1-hexene at 250 °C (1000 rpm), where the catalyst was ground to 150 µm (open points) and 300 µm (closed points). Weight fraction of: ◊ = Linear hexene isomers; □ = skeletal hexene isomers and △ = overall hexene depletion.

Therefore all experiments were completed at 1000 ppm with the catalyst ground to less than 150 µm to eliminate the effect of both internal and external mass transfer. The reaction progression was measured for 1-hexene and DMB respectively at 100, 150, 200 and 250 °C. A list of all the experiments that were completed to evaluate the kinetics for the dimerisation of hexene is shown in Table 3-2.

Table 3-2: Kinetic experiments completed.

T	m_{cat} (g)	V (L)
	DMB	
100 °C	5.0	0.15
150°C	7.7	0.17
200°C	6.0	0.19
250°C	5.7	0.22
	1-Hexene	
100 °C	5.1	0.16
150°C	7.2	0.18
	5.6	0.17
200°C	4.3	0.19
	5.1	0.21
	5.3	0.19
250°C	6.4	0.25
	8.0	0.25

3.2.3 Analysis

Samples were analysed by means of an Agilent Technologies 6890 gas chromatograph (GC) fitted with a flame ionisation detector (FID). Elutriation was established on a 50-m long Pona column with a 0.2 mm inner diameter and a 0.5 mm film thickness with N_2 as carrier gas at a flow rate of 25 ml/min. A split ratio of 100:1 was used. The initial column temperature was 40 ^{o}C, where it was held for 5 minutes, after which the temperature was ramped up to 300 ^{o}C at increments of 8 ^{o}C/min, where it was finally held constant for 5 minutes. The retention times of various hexene isomers were determined by injecting analytical grade standards from Sigma Aldrich: cis & trans 2-hexene (85%), 3,3-dimethyl-1-

butene (95%), 2-methyl-2-pentene (98%), 2,3-dimethyl-1-butene (97%), 2,3-dimethyl-2-butene (98%) and 2-ethyl-1-butene (95%). The hexene isomers were also confirmed using GC-MS, the possibility does however exist that some isomers are hidden due to overlapping.

The dimerised product cracked in a wide range of products, and C_4 to C_{13} olefins were detected. All the components elutriated before the tetradecane solvent, suggesting that the formation of trimer product was insignificant over the entire temperature range investigated. Overlapping with the tetradecane solvent which could mask the formation of oligomerised product was eliminated by the fact that the tetradecane weight fraction remained constant throughout all the experimental runs.

To differentiate between the cracked products, a GC-FID analysis was compared to the elutriation of the carbon numbers identified from a GC-MS (MS – mass spectrometry). The GC-MS was set to identify products from 20-300. Significant overlapping occurred for carbon numbers larger than C_9. Since the GC-MS could not be used for the analysis of every sample, the peak carbon numbers were related to the GC-FID residence times and from this a carbon number could be attributed, depending on the residence time of the peak through the column. A conservative residence estimate was used to identify each carbon number. The carbon distribution that resulted for the GC-FID analysis is shown in Table 3-3.

Table 3-3: Carbon analysis.

	GC Residence time (min)	
	Lower boundary	Upper boundary
C_4	0.00	2.04
C_5	2.04	3.03
C_6	3.03	4.45
C_7	4.45	8.00
C_8	8.00	10.50
C_9	10.50	12.50
C_{10}	12.50	14.30
C_{11}	14.30	15.70
C_{12}	15.70	18.60
C_{13}	18.60	22.50
C_{Other}	22.50	t_{end}

Due to the excessive overlapping of peaks, the GC-MS could not be used to distinguish between olefins, cyclics or aromatic molecules. Each one of these molecules could form from the dimerisation of 1-hexene over an acid catalyst (Figure 2-10). For this reason 1-hexene was dimerised to 80% total conversion of the hexene isomers and the product (boiling higher than 170 °C) was distilled and analysed, using GCxGC to determine the fraction of olefins, cyclics and/or aromatics. The GCxGC was done using a Pegasus 4D GCxGC system, supplied by Leco, Co. (St. Joseph, MI, USA), equipped with both TOF-MS and an FID detector. The primary column was a 50-m FFAP capillary column (0.20 mm internal diameter, *i.d.*, and 0.30-µm film thickness, *df*). The secondary column was a 2-m Rtx-5 column (0.1 mm *i.d.*, 0.1 µm *df*). The primary oven was programmed as follows: 35 °C for 1 min, ramped at 3 °C/min to 240 °C. The second oven followed the first oven program with a 10 °C offset. A duel jet thermal modulation system was used with an 8-second modulation period; 0.5 mL was injected using an Agilent Technologies 7683 auto injector. Hydrogen carrier gas was used at a constant flow of 1.3 mL/min. The split ratio was 400:1. Data collection for the TOF-MS and FID was at 100 spectra/sec.

3.3 Results & Discussion

3.3.1 Double bond and skeletal isomerisation

During oligomerisation, isomerisation and cracking occur simultaneously (Quann *et al.,* 1988). Since it has been shown that SPA is more prone to the oligomerisation of branched olefins (de Klerk, 2008), the rate of isomerisation is critical to describing the reaction rate. Previous work on the isomerisation of 1-hexene in the vapour phase indicated that isomerisation appeared to be step-wise: 1-hexene → methyl pentenes → dimethyl butenes (Hay *et al.*, 1945). If the hexene isomers identified throughout the progression of the reaction are plotted, a clear stepwise progression is seen in the formation of the isomers, shown in Figure 3-4. Initially only 1-hexene is present which disappears almost instantaneously from the bulk reaction mixture to form linear double bond isomers. Shortly after the appearance of double bond isomers, skeletal isomers are seen in the reaction mixture.

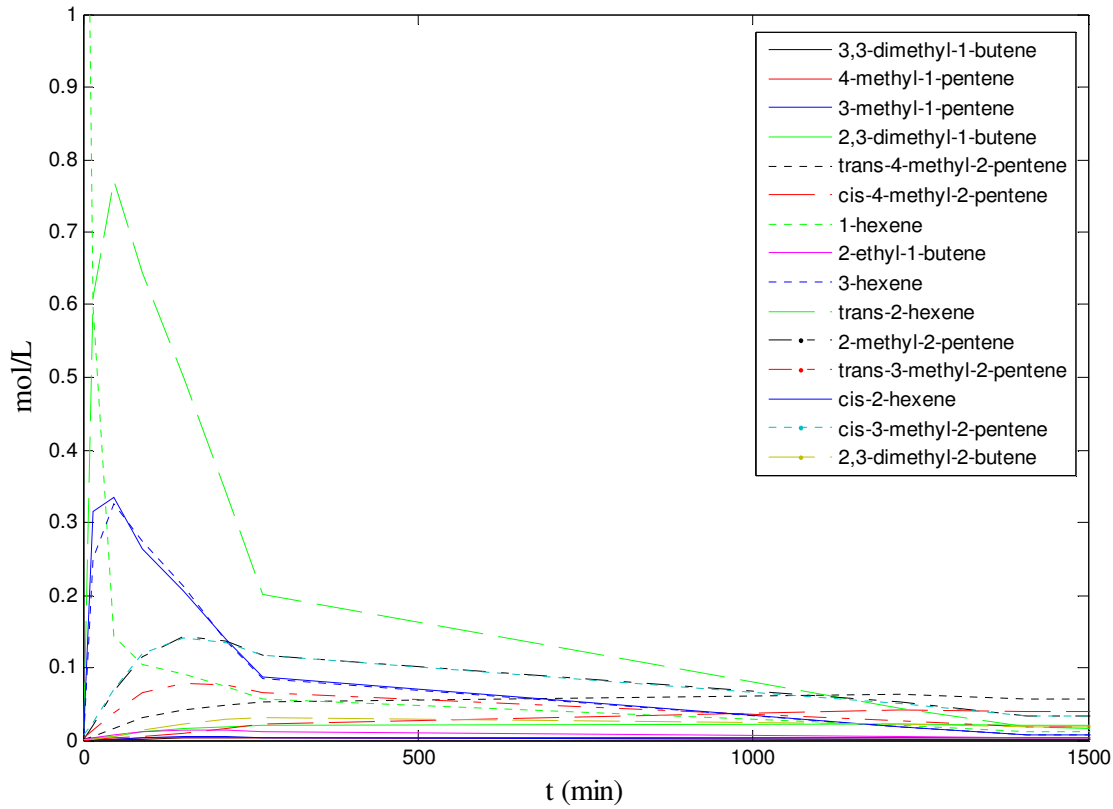

Figure 3-4: Hexene isomers identified by GC-FID during the dimerisation of 1-hexene at 200 °C.

The hexene isomers were further divided according to the degree of branching and the position of the double bond to identify differences in the reactivity of the different isomers. The grouping of the hexene isomers were done as described in Table 3-4.

Table 3-4: Groupings of hexene isomers

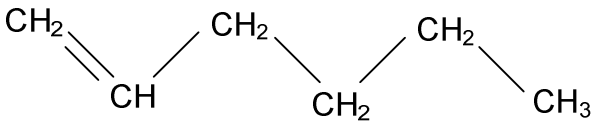	Linear hexenes, Figure 3-5 a)
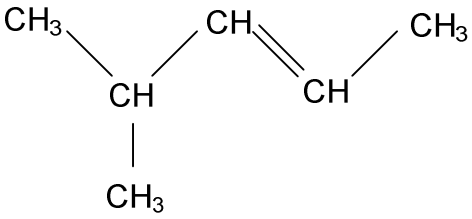	Beta disubstituted olefins (group A); where the double bond is located between two secondary carbons, e.g. trans-4-methyl-2-pentene, Figure 3-5 *b*).
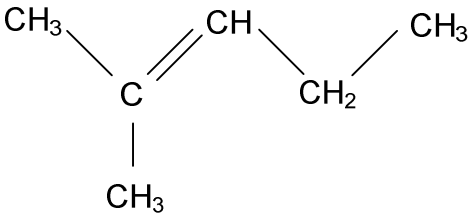	Tetra- and Trisubstituted olefins (group B); with the double bond between a secondary and tertiary carbon or situated between two tertiary carbons, e.g. 2-methyl-2-pentene; cis- and trans-3-methyl-2-pentene; 2,3 dimethyl-2-butene, Figure 3-5 *c*).
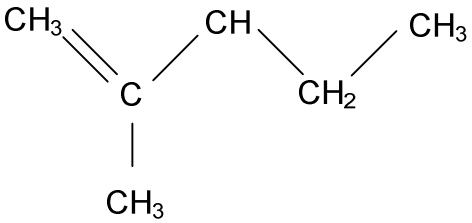	Mono substituted and alpha disubstituted olefins (group C); where the double bond is situated between a primary and tertiary carbon, e.g. 2,3-dimethyl-1-butene; 2-ethyl-1-butene, 3-methyl-1-pentene, Figure 3-5 *d*).

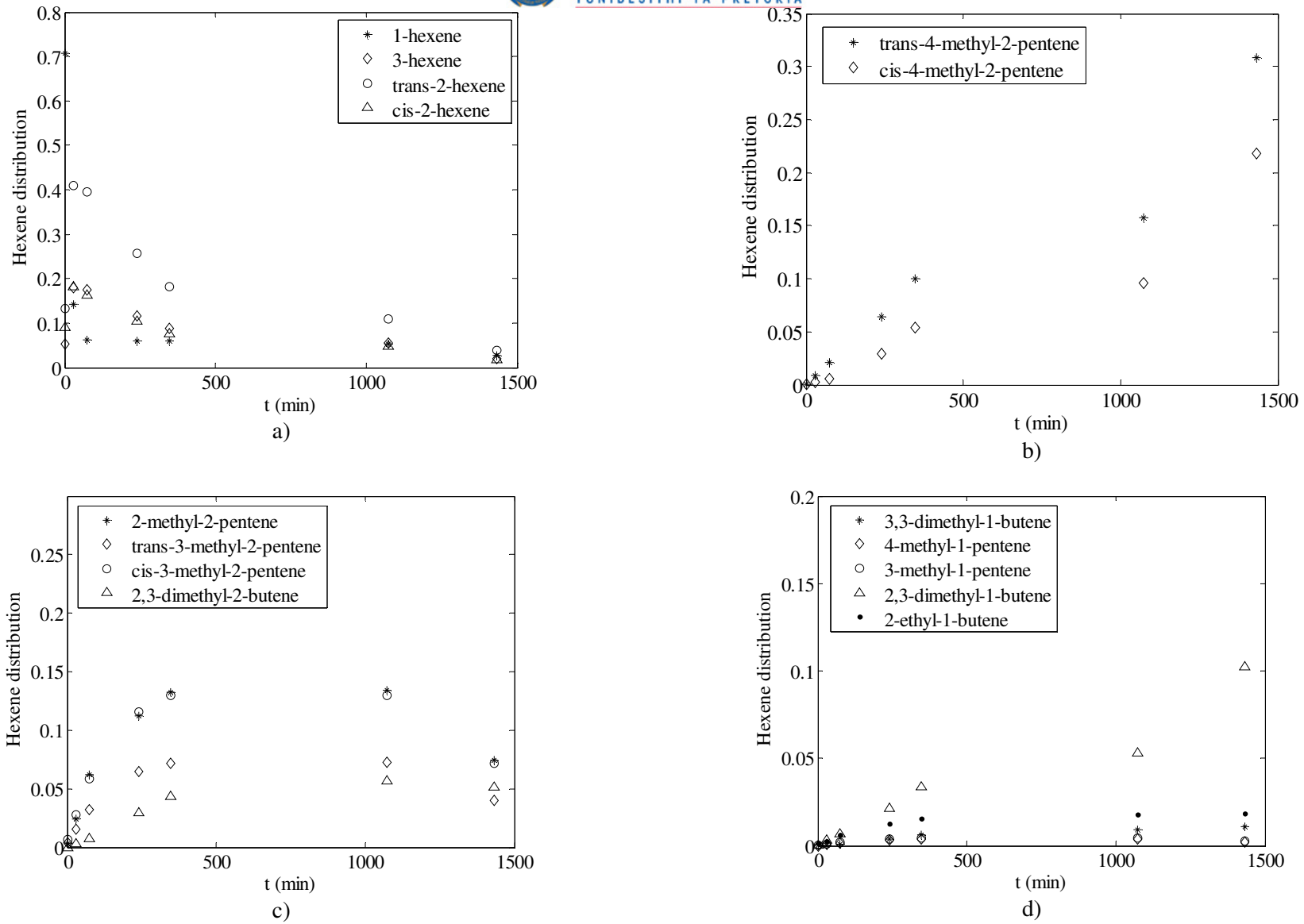

Figure 3-5: Isomers identified for 1-hexene dimerisation at 200 °C divided into *a)* linear hexenes, *b)* group A branched h*e*xenes, *c)* group B branched hexenes and *d)* group C branched hexenes.

As can be seen from Figure 3-5 linear hexenes are initially present to a much more significant extent than the branched hexenes, also the formation and subsequent depletion of branched hexenes is mostly localised with the formation of group B branched hexenes. Whereas group A and C skeletal isomers form to a lesser extent with little depletion afterwards. Skeletal isomerisation of olefins can either occur by methyl shift (Figure 2-11 *b))* or by the cracking of dimerised product (*isomerisation cracking*). The latter of the two was not seen in the early stages of the reaction. Branched hexenes were identified before the formation of C_{12}s for all experiments, indicating that the isomerisation of linear hexenes occurs by methyl shift. This is not to say that the dimerisation of linear hexenes does not occur, but rather that isomerisation occurs faster. It should also be noted that before a branched product can form from isomerisation cracking of two linear hexenes, skeletal isomerisation of the C_{12} product would first need to occur. From this work it is more evident that isomerisation occurs through methyl shift and not isomerisation cracking.

Throughout the investigation, linear hexenes seemed to convert irreversibly to skeletal isomers, with branched hexenes being more prominent toward the latter stages of the experiment. This indicates that the cracking of C_{12}s, to hexenes, results in the formation of branched hexenes, which indicates an equilibrium distribution between the dimerised product (C_{12}s) and the branched hexenes. If the dimerisation of linear hexenes occurs, the dimerised product will first need to isomerise before cracking to a branched product can be possible, Figure 3-6. This indicates that either linear hexene did not dimerise significantly or that the dimerised product can easily isomerise.

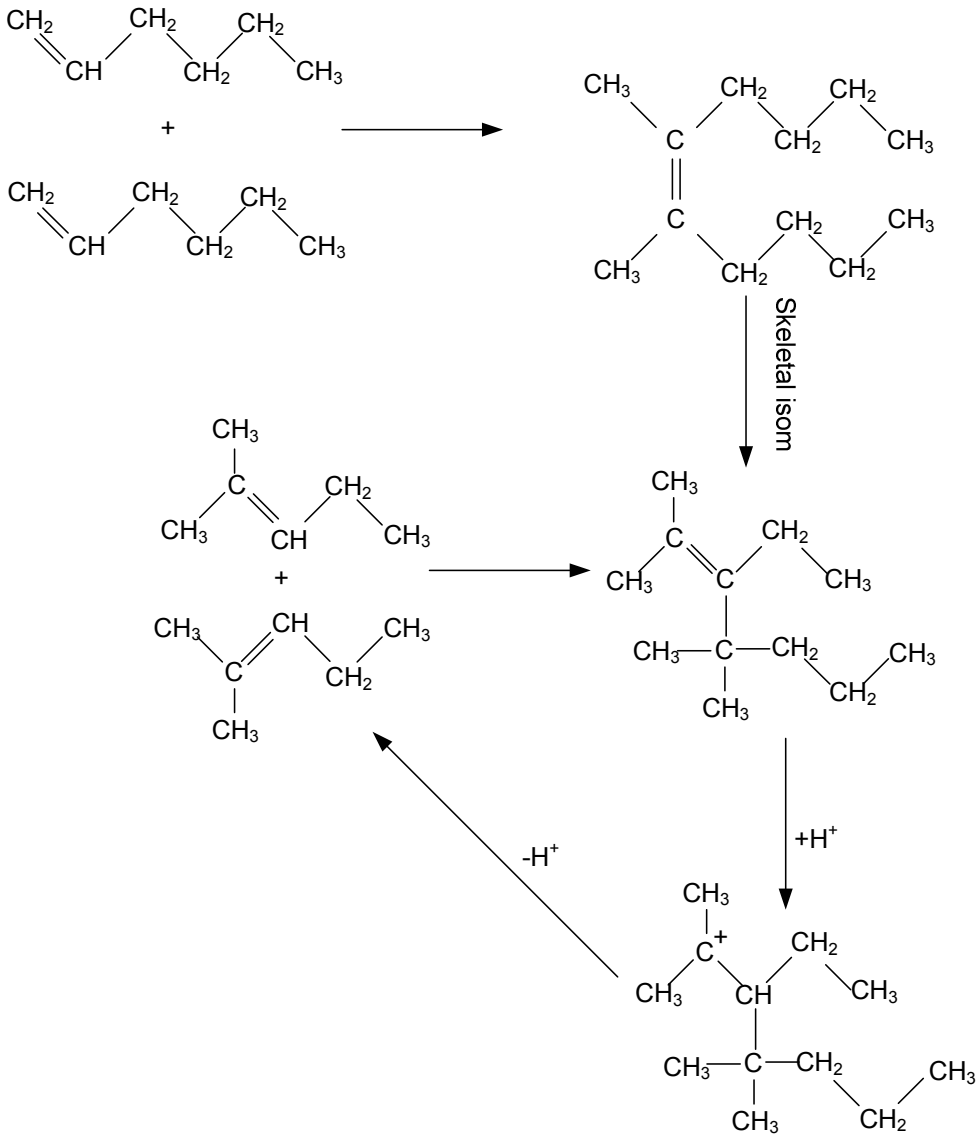

Figure 3-6: Cracking route of C_{12} product.

To determine whether the disappearance of the linear hexenes is due to the formation of skeletal isomers or due to the conversion to dimerised product, the depletion of all hexene isomers relative to the formation and depletion of linear hexenes and branched hexenes was studied, Figure 3-7. Since 1-hexene disappears quickly to the other linear isomers, all the linear hexenes were lumped together. The depletion of the hexenes was assumed to occur toward the formation of C_{12} dimers, merely to illustrate the rate of reaction, not the product selectivity. Linear hexenes in this instance are a grouping of all linear hexenes, 1-hexene included. Initially little depletion of hexene isomers was seen, with an inflection point evident for the depletion of hexenes where the formation of branched hexenes reached a maximum

(Figure 3-7, with the dotted line indicating the inflection point). This indicates that the depletion of hexenes to dimerised product occurs to a greater extent once skeletal isomers have been formed.

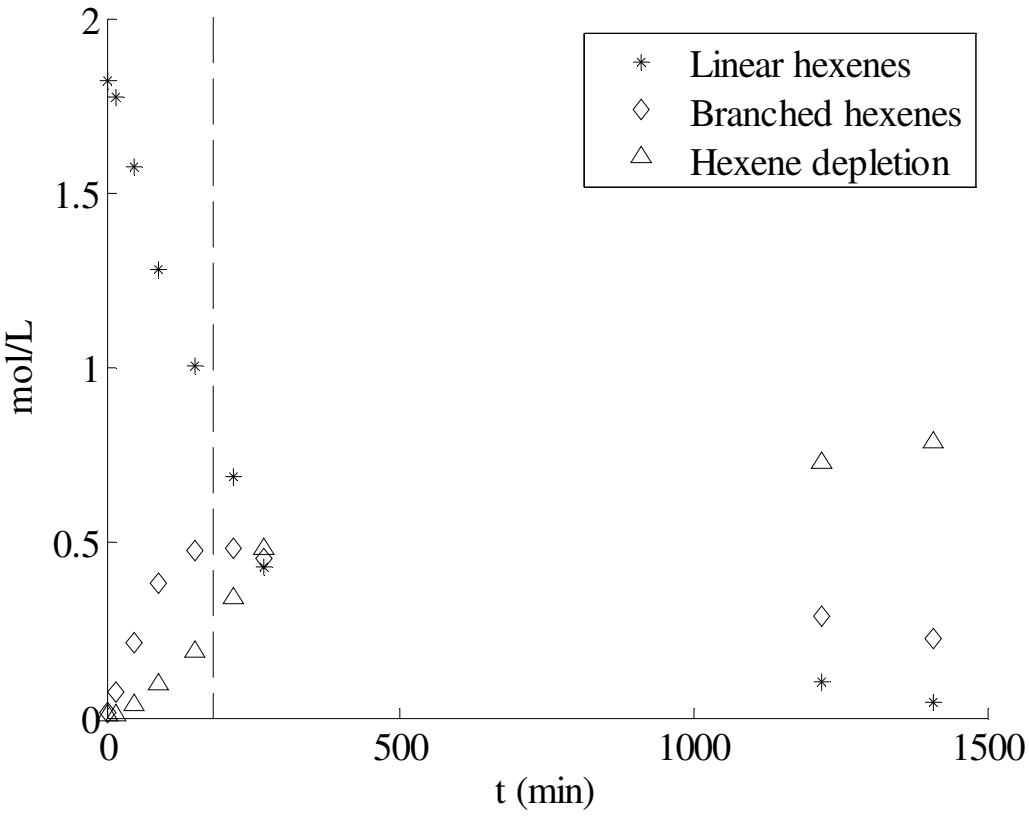

Figure 3-7: The reaction progression for 1-hexene dimerisation with reference to linear hexenes, branched hexenes and hexene depletion (dimerisation) at 200 °C.

If 1-hexene is fed into the reactor, the interaction between linear hexenes, branched hexenes and dimerised product is convoluted. It is not simple to determine whether the oligomerised product is formed from the dimerisation of branched hexenes or the co-dimerisation between the linear and branched isomers. For this reason, new insights into the dimerisation of hexene were gained from the dimerisation of 2,3-dimethyl-2-butene (DMB) with reference to 1-hexene dimerisation (especially while using a reaction model). The relative formation of hexene isomers and dimerised product can be correlated to give a clearer indication of the isomers that are most reactive. Figure 3-8 shows the formation of hexene isomers seen during the dimerisation of DMB over SPA. The hexenes isomers identified are dominated by two isomers: *1)* DMB and *2)* 2,3-dimethyl-1-butene (DM1B, double bond isomers).

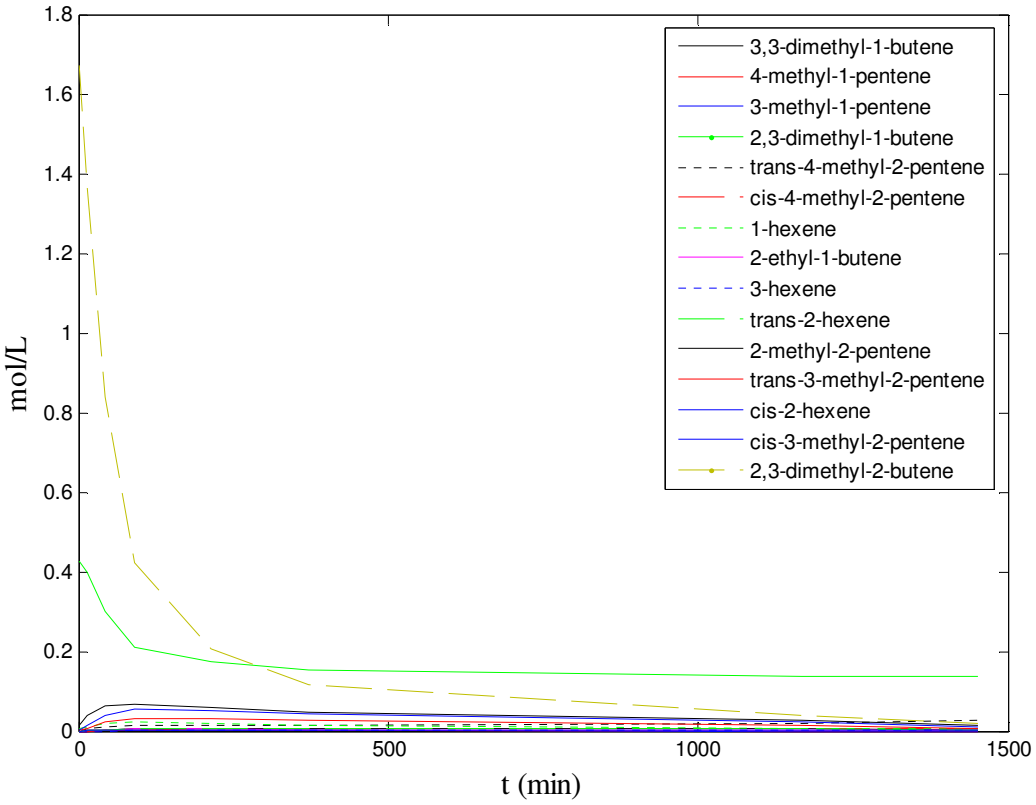

Figure 3-8: Hexene isomers identified for the dimerisation of DMB at 200 °C.

The distribution of hexene isomers is again separated based on the position of the double-bond and is shown in Figure 3-9. It can be seen that linear hexenes are formed to an insignificant extent. Not only is the formation of linear hexenes limited but also the formation of other skeletal hexene isomers does not occur significantly. This indicates that methyl shift occurs irreversibly and that the formation of other hexene isomers, when dimerising DMB, only results from the cracking of oligomerised product.

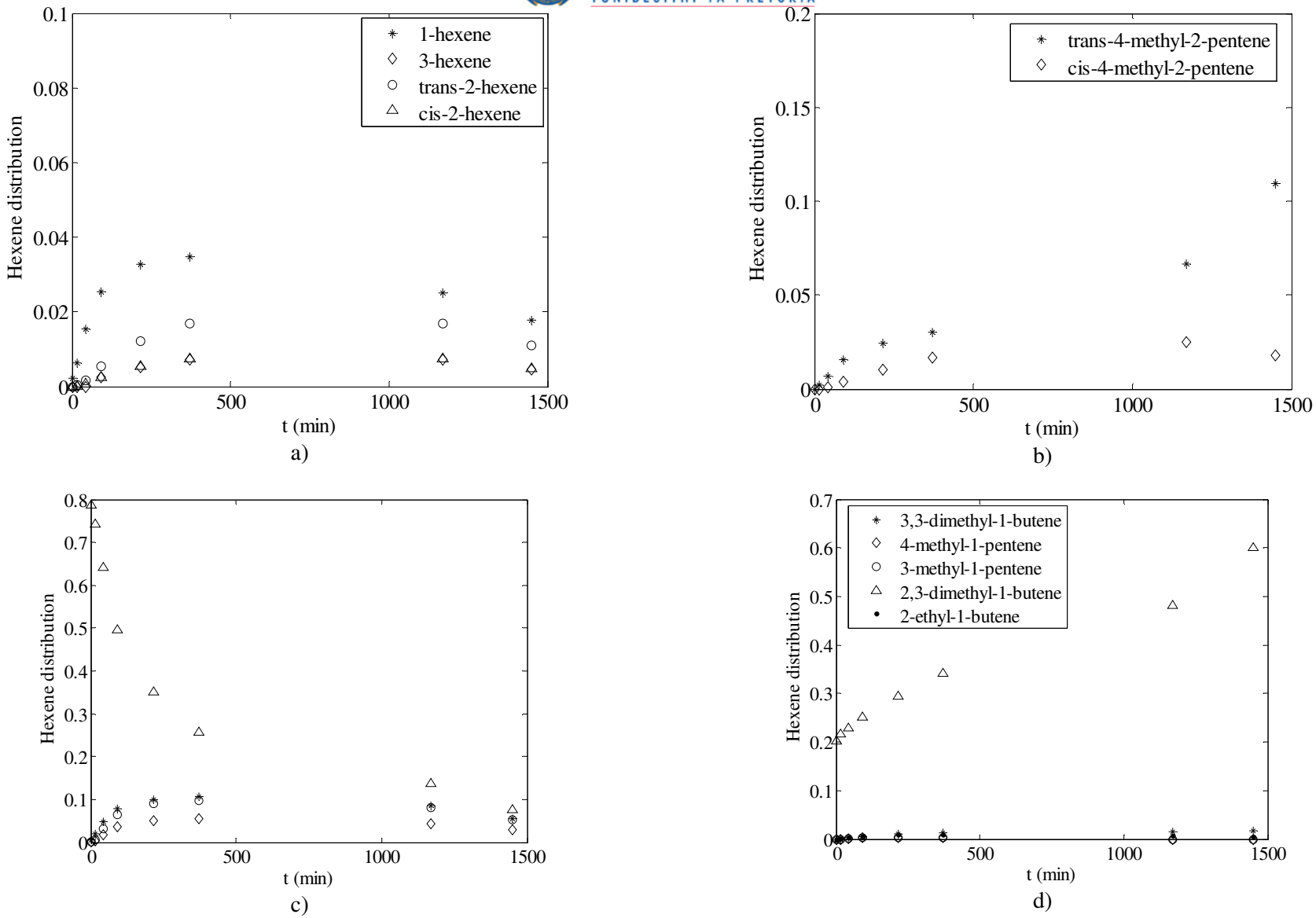

Figure 3-9: Isomers identified for DMB dimerisation at 200 °C divided into *a)* linear hexenes, *b)* group A branched hexenes, *c)* group B branched hexenes *d)* group C branched hexenes.

If the depletion of hexene isomers for the dimerisation of DMB is plotted, a steadier depletion of the hexene isomers to dimerised product is observed. It is also evident that there is no inflection point in the depletion of hexenes, indicating a single-step depletion of hexenes. The formation of linear hexenes is also seen to be insignificant with respect to the other hexene isomers and dimerised product; these trends were observed over the entire temperature range.

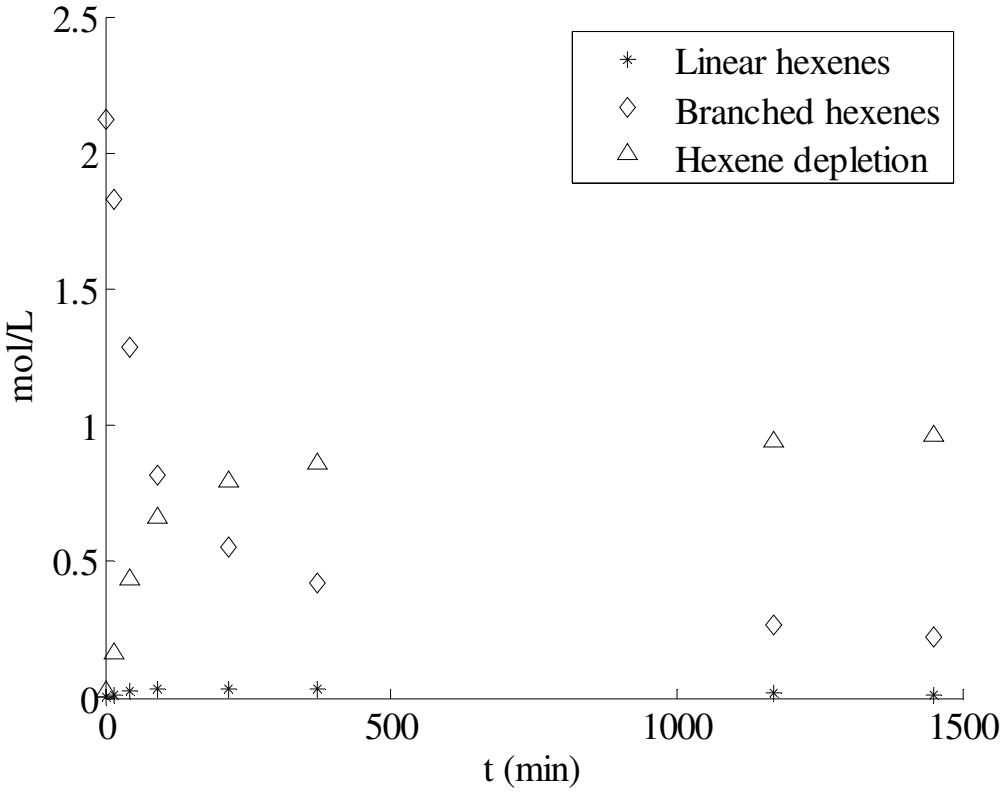

Figure 3-10: The reaction progression for DMB dimerisation with reference to linear hexenes, branched hexenes and hexene depletion (dimerisation) at 200 °C.

From Figure 3-8 and Figure 3-9 it seems that the double bond isomer of DMB, DM1B, forms quickly and the then remains constant. This might indicate that the isomer is non-reactive, or that an equilibrium distribution prevails. If the equilibrium distribution of hexene isomers are determined using an RGIBS reactor from Aspen^{TM}, the distribution in Table 3-5 is obtained. This shows that at 200 °C the equilibrium distribution of DMB and DM1B favours DM1B, whereas at lower temperatures DMB is favoured.

Table 3-5: Equilibrium distribution of hexene isomers from RGIBS reactor (Aspen™)

	100 °C	150 °C	200 °C	250 °C
1-hexene	0.1%	0.2%	0.3%	0.5%
cis-2-hexene	0.6%	1.0%	1.5%	2.1%
trans-2-hexene	1.6%	2.3%	3.1%	3.8%
cis-3-hexene	0.2%	0.4%	0.6%	0.8%
trans-3-hexene	1.0%	1.5%	2.0%	2.4%
2-methyl-1-pentene	4.6%	5.7%	6.6%	7.2%
3-methyl-1-pentene	0.3%	0.5%	0.8%	1.1%
4-methyl-1-pentene	0.2%	0.3%	0.4%	0.5%
2-methyl-2-pentene	15.0%	13.4%	11.8%	10.5%
3-methyl-cis-2-pentene	18.9%	20.1%	20.5%	20.3%
4-methyl-cis-2-pentene	1.2%	1.7%	2.2%	2.6%
4-methyl-trans-2-pentene	2.6%	3.2%	3.7%	4.2%
2-ethyl-1-butene	2.1%	2.9%	3.7%	4.4%
2,3-dimethyl-1-butene	22.9%	23.5%	23.7%	23.7%
3,3-dimethyl-1-butene	0.1%	0.1%	0.2%	0.2%
2,3-dimethyl-2-butene	28.6%	23.3%	19.0%	15.6%

To determine if the DM1B is unreactive or if an equilibrium distribution is present, more data is required. If the distribution of DMB and DM1B is plotted for the reaction rate of DMB of SPA at 150 °C, Figure 3-11, it is evident that DMB is favoured. As such the distribution of the DMB and DM1B can be attributed to the equilibrium distribution of isomers.

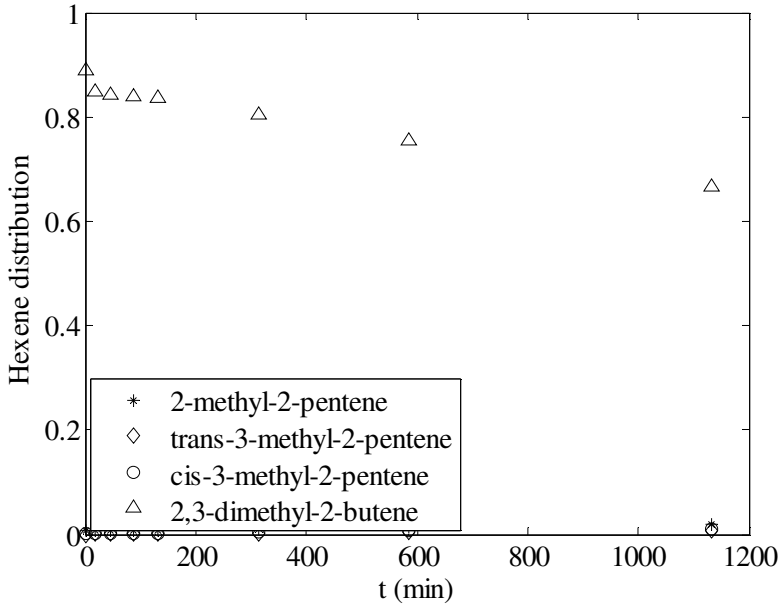

a)

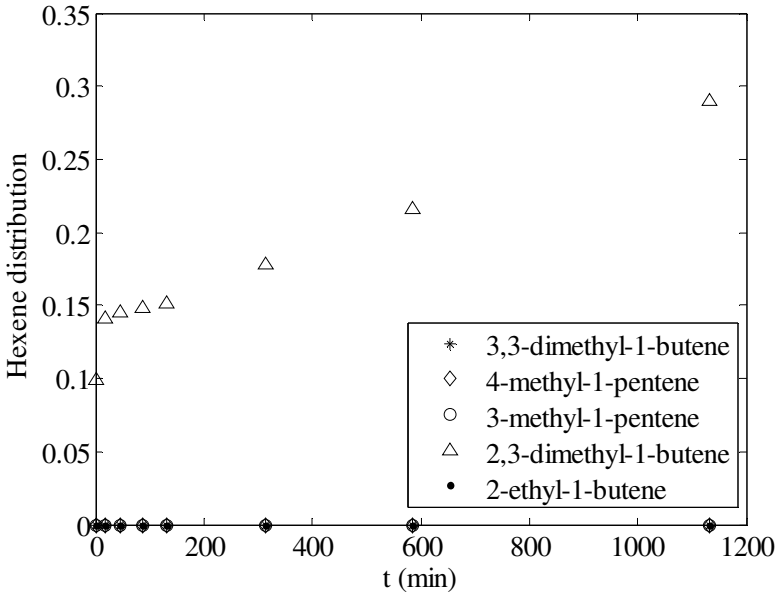

b)

Figure 3-11: Distribution of DMB at 150 °C for *a*) group B branched hexenes and *b)* group C branched hexenes (an insignificant amount of linear hexenes and group A hexenes was observed at 150 °C for the dimerisation of DMB over SPA).

3.3.2 Dimerised and cracked products

In the previous section the emphasis was placed on the formation of hexene isomers with little emphasis on the product spread. As cracking is prominent over SPA, the chain length of the resulting product is important to quantifying the quality of the produced fuel, Section 2.1. The formation of the different carbon numbers identified from GC-MS/FID is shown in Figure 3-12. For each carbon number a bar graph is shown; each bar indicates the chronological formation of the product from the onset of the reaction (first bar) to the end of the experiment (last bar).

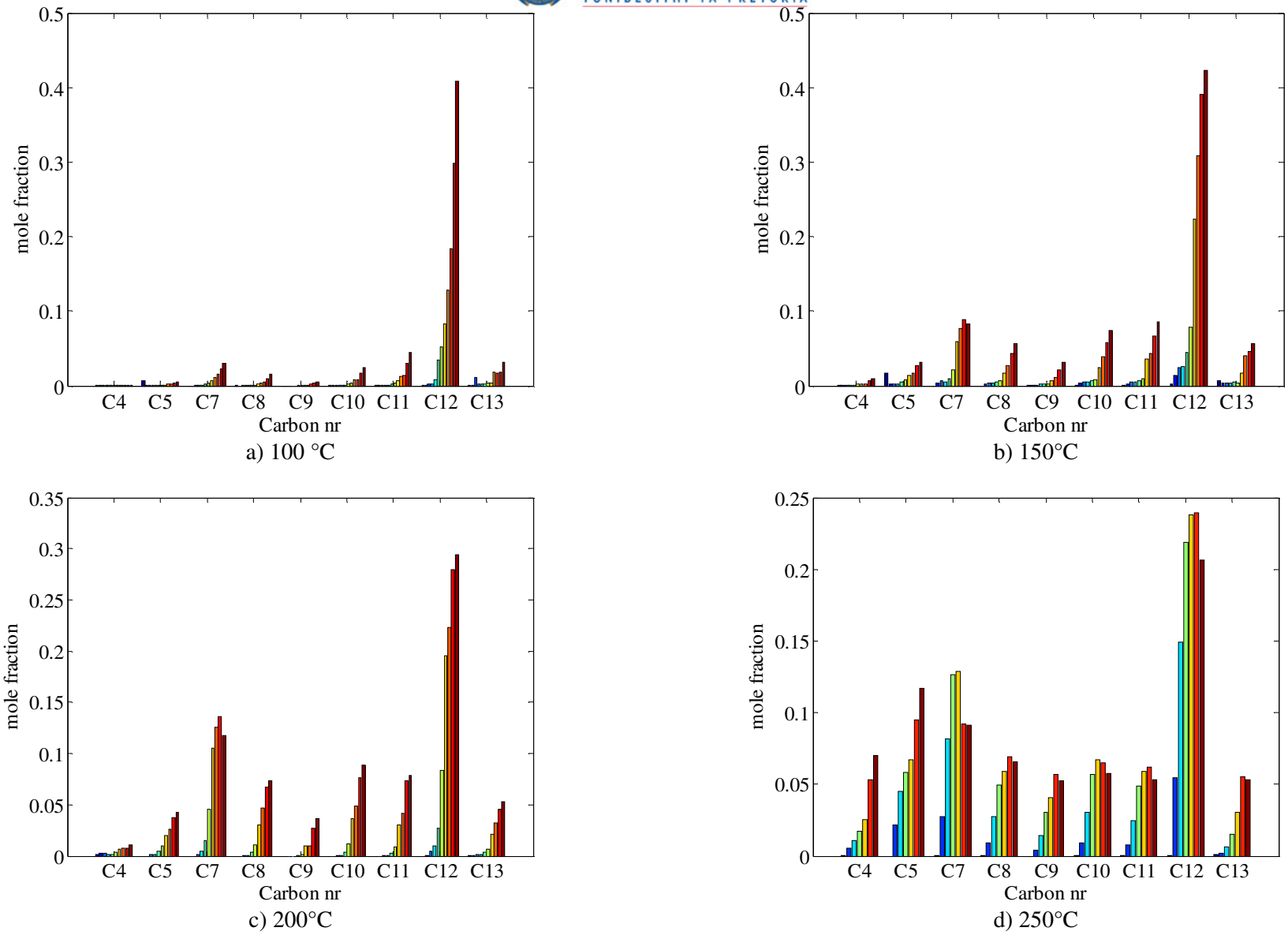

Figure 3-12: Formation of oligomerised and cracked products for 1-hexene dimerisation.

It is notable from the GC-MS analysis of the product that the reaction of 1-hexene over SPA is limited to the formation of dimerised product, with no trimerised product identified. It is clear from Figure 3-12 that a much higher selectivity toward the formation of dimers is seen at lower temperatures, with little cracking observed. As the temperature increases, the carbon number distribution evens out. A simplistic method of evaluating the distribution of the cracked product at each interval is to evaluate the concentration of each carbon number with respect to the total hexene depletion to C_{12}s, D, as shown in Equation 3-1.

$$K_{eq} = \frac{C_x}{D} \qquad 3\text{-}1$$

where C_x is the concentration of carbon number x and D is the total hexene depletion expressed as C_{12} formation.

This assumes that cracking occurs after dimerisation, which is in line with the work of De Klerk (2005b) who states that the cracking of hexenes will only become significant above 275 °C. Therefore in this investigation, only the cracking of olefins heavier than C_6 should occur. For this reason, cracking will only occur once dimerisation has occurred. The resulting distribution of each carbon number, from the start to the end of each experiment, is shown in Figure 3-13. Both Figure 3-12 and Figure 3-13 indicate a higher selectivity toward cracked products at higher temperatures, with lower temperatures being more selective toward the dimerisation of hexene. Interestingly, the distributions of dimerised and cracked products are relatively flat for each carbon number from the onset of the reaction. This indicates that once dimerisation has occurred, the cracking and co-dimerisation that follow are essentially instantaneous with an *equilibrium* distribution. Similar trends are evident for the dimerisation of DMB, shown in Appendix 8.1 (Figure 8-1 and Figure 8-2).

The observation that the carbon number distribution evens out quickly suggests that it is not possible to isolate the formation of dimerised product at a minimal formation of cracked products. This indicates that the gasoline to diesel/jet fuel distribution (due to both cracking and co-dimerisation) for the dimerisation of hexenes will depend on the reaction temperature, not on the residence time in the reactor.

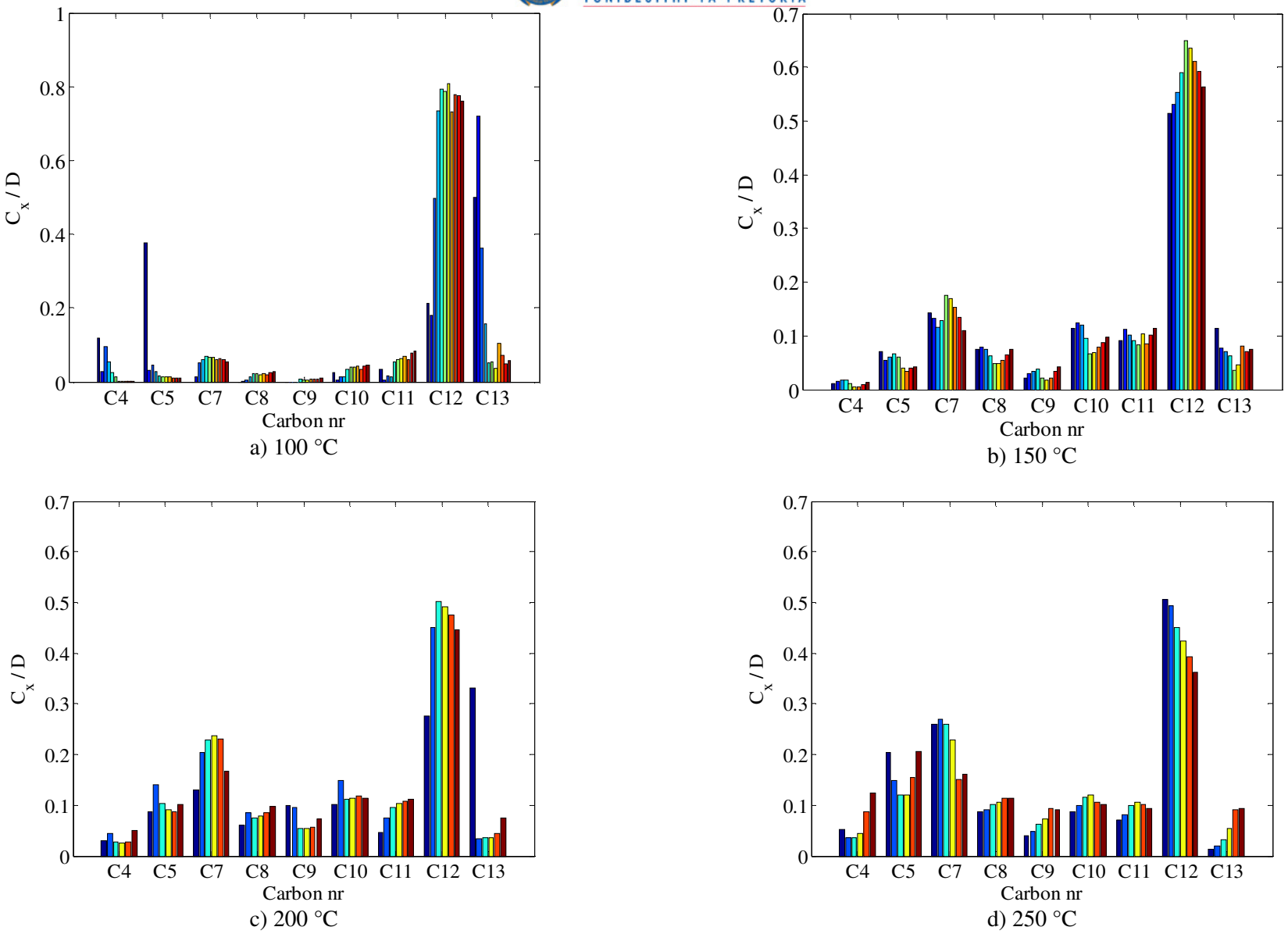

Figure 3-13: Distribution of cracked and dimerised product for 1-hexene dimerisation.

To assess the product spread further, a GCxGC analysis was done on the product from 1-hexene dimerised product (boiling above 170 °C) at 100, 150 and 250 °C (unfortunately, data could not be collected at 200 °C). The GCxGC analysis indicated that even at 100 °C the formation of cyclics and aromatics was evident, increasing as the temperature increased (Table 3-6 and Figure 8-3 in the appendix). Due to the increased cracking at higher temperatures, the distribution of observed carbon numbers expanded at higher temperatures. It was not possible, to analyse each sample using the GCxGC, so the formation of cyclics/aromatics could not be incorporated into the kinetic evaluation of 1-hexene dimerisation.

The formation of cyclic and aromatic compounds over SPA is by no means a new occurrence and has been noted by Ipatieff (1935) and Ipatieff and Corson (1936) for the oligomerisation of propylene and ethylene respectively. The formation of aromatics for the oligomerisation of short chain olefins over SPA is however not so conclusive. A GC x GC analysis that was completed for the oligomerised product from the oligomerisation of C_3 and C_4 olefins over SPA showed that cyclic molecules was present in the product (Van der Westhuizen *et al.*, 2010). Although cyclics is a precursor to the formation of aromatics, no aromatics was observed in the investigation. These investigations focused on the oligomerisation of short chain olefins, whereas 1-hexene was oligomerised in this instance. An investigation that observed aromatics while oligomerising 1-hexene, however using USY Zeolite, was Anderson *et al.* (1991). No other reference could be found to the formation of aromatics over SPA for 1-hexene oligomerisation. It is however not within the scope of this research to investigate the formation of aromatics from 1-hexene, but rather focus on the oligomerisation of 1-hexene.

Table 3-6: Product spread for GCxGC at different temperatures.

Carbon Number	Olefins	Cyclic Olefins	Total
	W %	W %	W %
C_9	0.03	0.00	0.03
C_{10}	5.71	0.02	5.73
C_{11}	4.54	0.18	4.72
C_{12}	64.42	1.86	66.28
C_{13}	7.88	0.27	8.15
C_{14}	1.27	0.32	1.60
C_{15}	0.12	0.09	0.21
C_{16}	0.34	0.09	0.43
C_{17}	0.44	0.40	0.85
C_{18}	2.16	3.80	5.96
C_{19}	0.13	0.52	0.65
C_{20}	0.00	0.06	0.06
C_{21}	0.00	0.00	0.00
		Light material < C_8	0.05
		Aromatics	5.29
Total	87.04	7.62	100.0

a) 100 °C

Carbon Number	Olefins	Cyclic Olefins	Total
	W %	W %	W %
C_9	0.00	0.04	0.04
C_{10}	1.32	0.05	1.37
C_{11}	13.22	0.53	13.74
C_{12}	45.35	0.41	45.75
C_{13}	14.59	1.94	16.53
C_{14}	3.06	0.70	3.75
C_{15}	1.42	0.36	1.78
C_{16}	1.42	0.80	2.22
C_{17}	3.44	0.67	4.11
C_{18}	2.40	3.52	5.92
C_{19}	0.00	0.68	0.68
C_{20}	0.00	0.89	0.89
C_{21}	0.00	0.00	0.00
		Light material < C_8	0.03
		Aromatics	3.18
Total	86.21	10.58	100.0

b) 150 °C

Carbon Number	Olefins	Cyclic Olefins	Total
	W %	W %	W %
C_9	0.03	0.00	0.03
C_{10}	0.70	0.05	0.74
C_{11}	7.45	0.71	8.16
C_{12}	32.62	4.49	37.12
C_{13}	9.66	2.38	12.04
C_{14}	4.26	5.88	10.14
C_{15}	1.31	3.39	4.71
C_{16}	1.08	2.34	3.41
C_{17}	0.40	2.61	3.01
C_{18}	0.36	4.01	4.37
C_{19}	0.00	0.97	0.97
C_{20}	0.00	0.36	0.36
C_{21}	0.00	0.08	0.08
		Light material < C_8	0.08
		Aromatics	14.78
Total	57.86	27.28	100.0

c) 250 °C

3.4 Kinetic model

To extract the reaction progression of the dimerisation of 1-hexene further, a kinetic model can be used to compensate for reactivity differences between hexene isomers. To model the reaction kinetics for the dimerisation of 1-hexene, the reaction sequence was depicted with respect to linear hexenes (A), branched hexenes (B) and hexene depletion to dimerised product (D) as shown in Figure 3-14. For the determination of the reaction progression various groupings and routes were evaluated to determine which gave the most successful prediction of the reaction rate, the reaction route depicted in Figure 3-14 gave the best description of the oligomerisation kinetics.

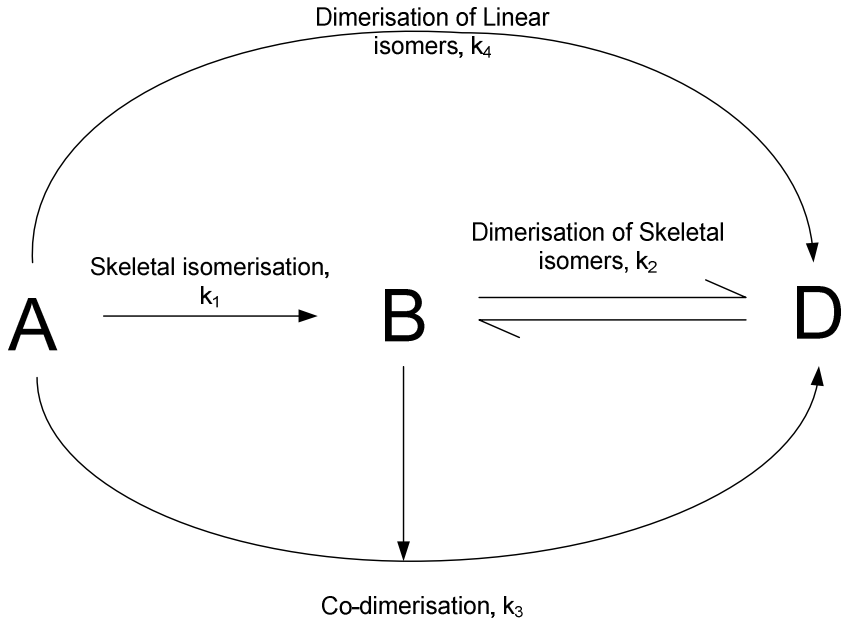

Figure 3-14: Reaction mechanism for hexene dimerisation.

Due to the almost instantaneous disappearance of 1-hexene by double bond isomerisation, all the linear hexenes could be successfully incorporated into a kinetic model as only linear hexenes (A). Even though some of the hexene isomers formed during the dimerisation of DMB seemed non-reactive (especially the group C isomers that formed to an insignificant extent), the incorporation of extra parameters to model this occurrence would only be justified if the simplified model shown in Figure 3-14 could not describe the rate of dimerisation of 1-hexene/DMB for all reaction conditions.

If double bond isomerisation is incorporated in the reaction path it is evident that the rate of double bond isomerisation far outweighed the other rate constants (Schwarzer *et al.*, 2009).

Essentially only an equilibrium constant is needed to predict the distribution of linear hexenes, as such to simplify the amount of kinetic parameters fitted to the experimental data the linear hexenes were lumped together. It is important to note that the reaction mechanism proposed in Section 2.6.2 focused extensively on the phosphoric acid ester forming with an alpha olefin, the literature focused on short chain olefins where the ester will only form with regards to an alpha olefin. For hexene oligomerisation this is not necessarily true, especially if the reaction rate of DMB is to be accounted for Figure 3-10.

Another possibility is that the rate of sorption limits the reaction rate, the first attempt at modelling the reaction rate was assuming a first order rate constant ($r_a = -kC_a$) as would be the case for sorption into another phase (Schwarzer *et al.*, 2009). This method of did not give a poor description of the reaction progression. To however reconcile all the reaction data (100 - 250 °C) the use of an elementary reaction order (second order kinetics), as would be true for a rate controlled reaction rate, improved the achieved fitting.

As such the reaction rate was modelled by using an elementary kinetic model shown in Equations 3-2 to 3-4, where k_1 is the rate of skeletal isomerisation, k_2 the dimerisation of skeletal/branched isomers (DBH), k_3 the co-dimerisation of linear and branched hexenes (CD) and k_4 the dimerisation of linear hexenes (DLH).

$$\frac{dC_A}{dt} = m_{cat}\left(-k_1 C_A - k_3 C_A C_B - k_4 C_A^2\right) \qquad 3\text{-}2$$

$$\frac{dC_B}{dt} = m_{cat}\left(k_1 C_A - k_2 C_B^2 + \frac{k_2}{K_{eq}} C_D - k_3 C_A C_B\right) \qquad 3\text{-}3$$

$$\frac{dC_D}{dt} = m_{cat}\left(k_2 C_B^2 - \frac{k_2}{K_{eq}} C_D + k_3 C_A C_B + k_4 C_A^2\right) \qquad 3\text{-}4$$

Where C is the concentration of A, B and D respectively; t is the time in min; m_{cat} is the weight concentration of catalyst; k_x is the rate constant and K_{eq} is the equilibrium distribution constant between branched hexenes and dimerised product. The optimisation of the kinetic parameter proved troublesome, particularly in view of the play-off between the CD, DLH and DBH with respect to the dimerisation of either 1-hexene or DMB. For this reason the kinetic

parameters were fitted for all the experimental data at one temperature, i.e. both the 1-hexene and DMB experimental data at a fixed temperature were used to fit the kinetic parameters, by minimising the absolute average relative error (AARE) for all the data gathered at that temperature (Equation 3-5).

$$AARE = \sum_{l} \sum_{n}^{A-D} \sum_{m} \left(\frac{\left| C_{\Pr edicted,l,n,m} - C_{Experimental,l,n,m} \right|}{C_{Experimental,l,n,m}} \right) \qquad 3\text{-}5$$

where *l* is the experiments completed at each temperature; *n* is A, B and D respectively and *m* is the data measured at each time interval.

After the optimisation of the kinetic parameters it became clear that DLH did not occur to a significant extent, and that only DBH and CD had to compensated for in order to model the experimental data. The resulting kinetic description for the experiments that were completed from 100-250 °C is shown for both 1-hexene and DMB in Figure 3-15 *a) - h)*. The kinetic fit of the experimental data allowed a good prediction of the formation and depletion of linear and branched hexenes and the resulting total depletion of hexenes for both 1-hexene and DMB dimerisation, especially taking into account that the same kinetic parameters were used to describe the reaction rate for both 1-hexene and DMB as the initial reagent. This also corroborates the inclusion of group C skeletal isomers into B.

With an increase in temperature, a more pronounced formation is seen in branched hexenes for 1-hexene dimerisation. A distinct maximum is also seen in the formation of branched hexenes at higher temperatures (Figure 3-15 *d)*), suggesting that the rate of formation of branched hexenes is more pronounced at higher temperatures.

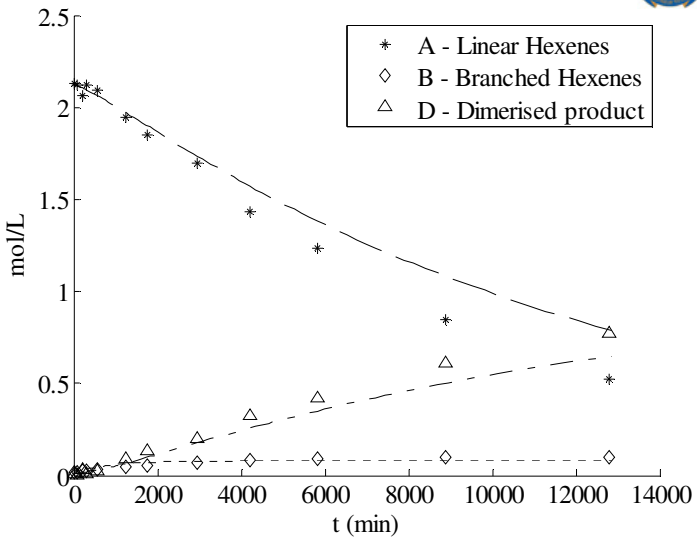

a) 1-Hexene, 100 °C

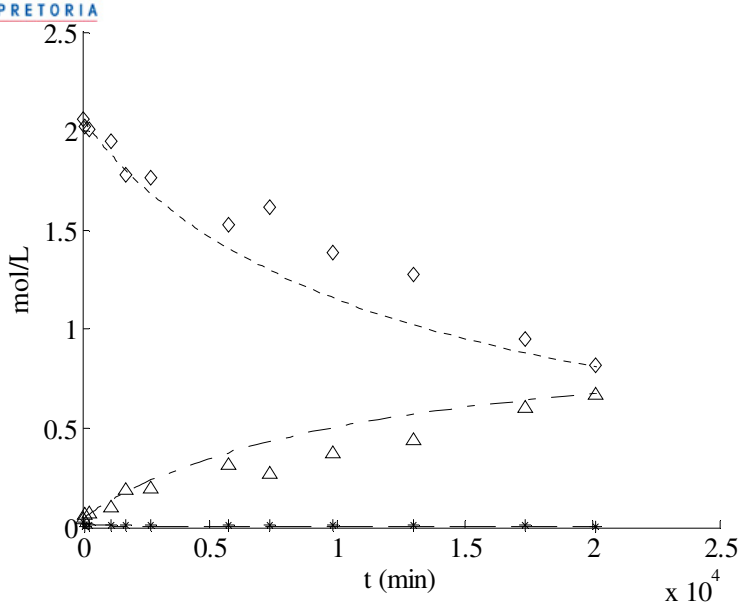

e) DMB, 100 °C

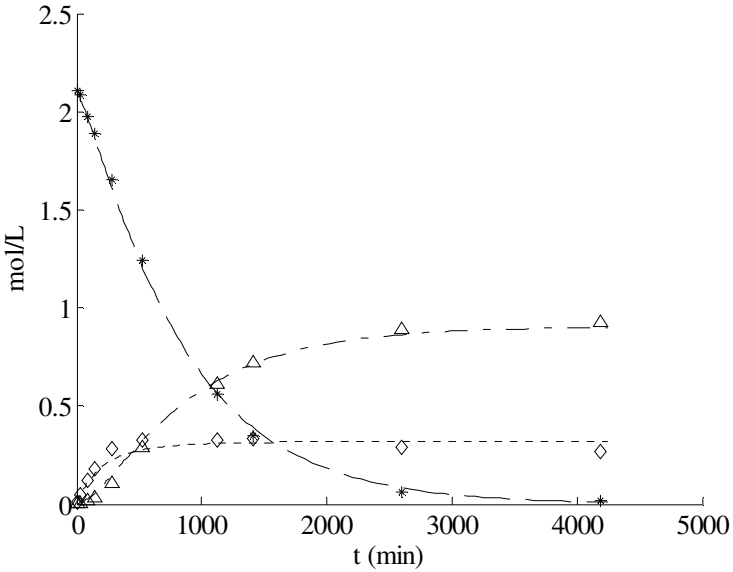

b) 1-Hexene, 150 °C

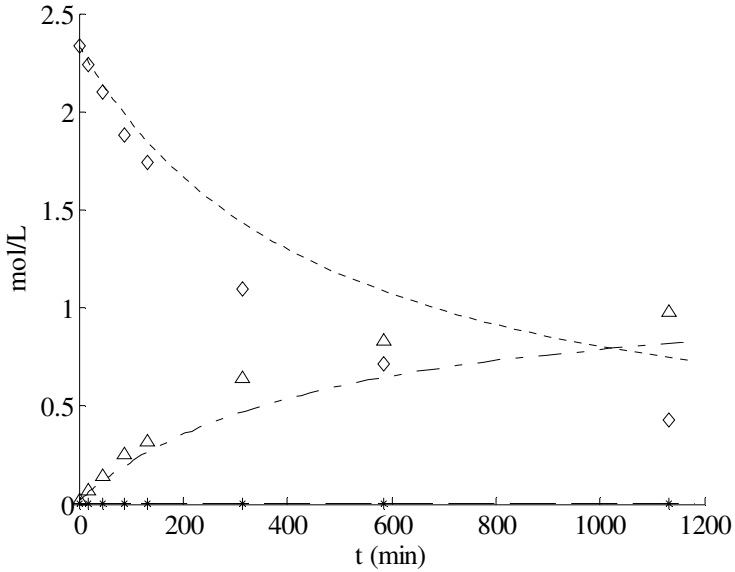

f) DMB, 150 °C

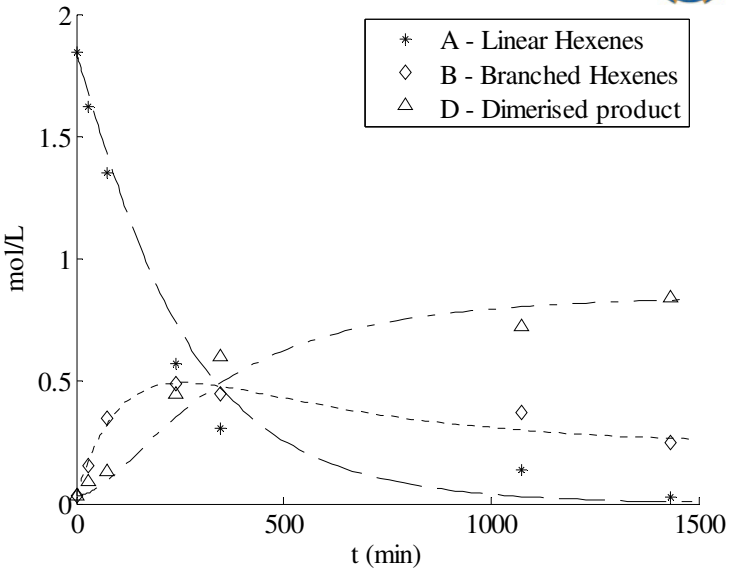

c) 1-Hexene, 200 °C

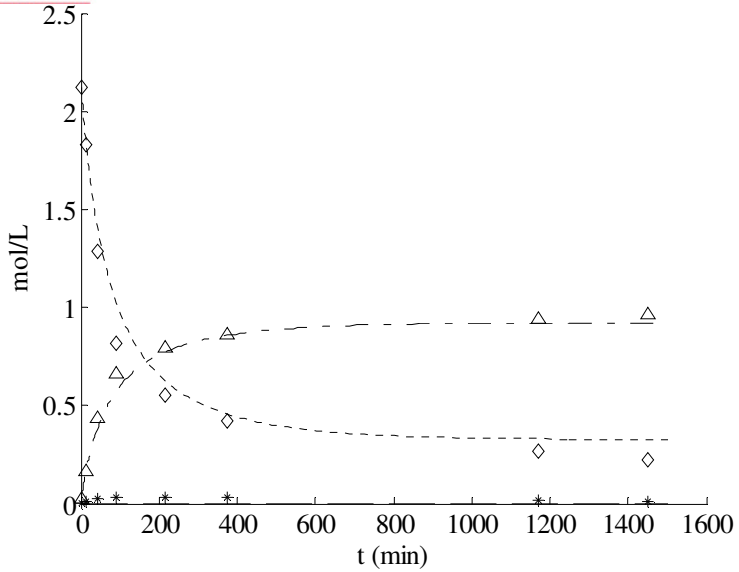

g) DMB, 200 °C

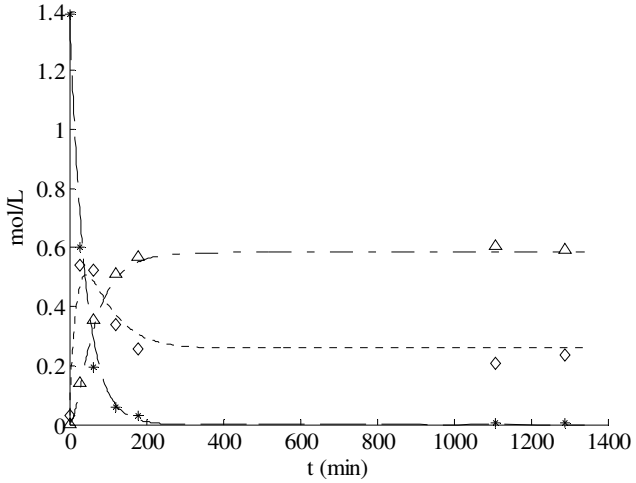

d) 1-Hexene, 250 °C

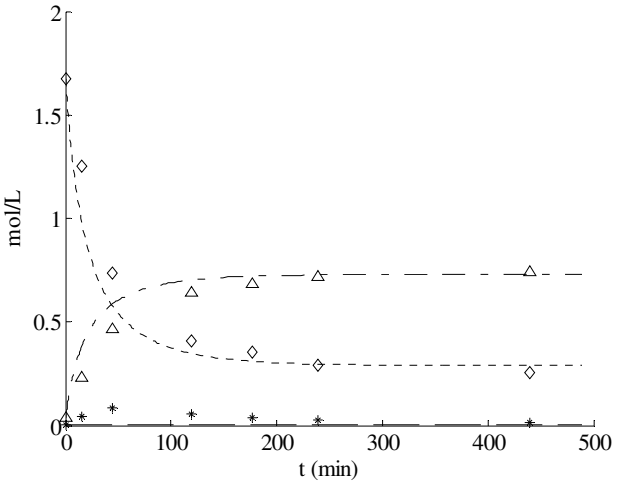

h) DMB, 250 °C

Figure 3-15: Kinetic fit of the dimerisation of 1-hexene, a) – d), and DMB, e) – h), with * - linear hexenes, ◊ - branched hexenes and △ - total hexene depletion.

To account for the temperature dependence of the rate constant, an Arrhenius relationship (Equation 3-6) can be used.

$$\ln(k_x) = \ln(k_{x,o}) + \frac{E_a}{RT} \qquad 3\text{-}6$$

where $k_{x,o}$ is the pre-exponential constant; T is the temperature in K and E_a is the activation energy.

The resulting temperature dependence of the kinetic parameters is shown in Figure 3-16.

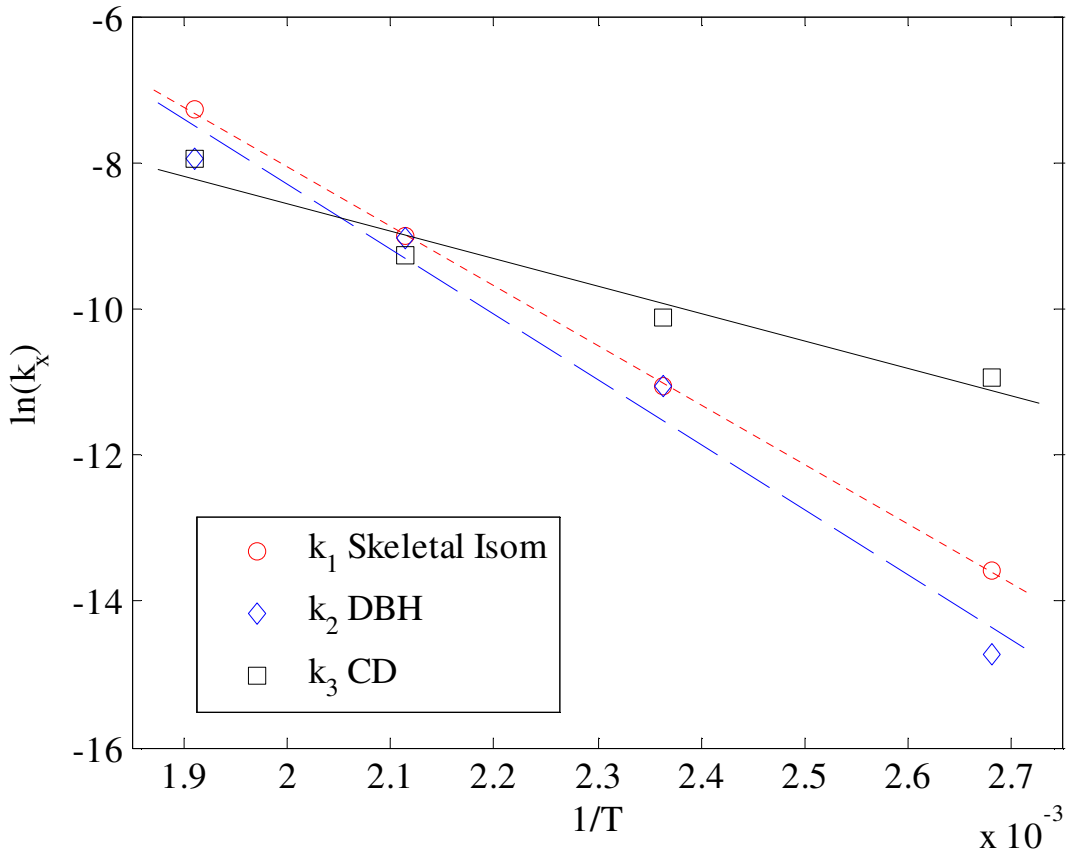

Figure 3-16: Arrhenius relationship of fitted kinetic parameters, where the rate constant is for the various steps given in Figure 3-14, k_1 – skeletal isomerisation, k_2 – DBH and k_3 – CD.

It is evident from the Arrhenius relationship that at low temperatures (100 – 150 °C), dimerisation (either by DBH or CD) is limited by the rate of skeletal isomerisation. The large activation energy for skeletal isomerisation has the result that at higher temperatures (200 – 250 °C) the dimerisation of hexenes can occur more freely.

The modelling of the reaction rate does not cover what transpires in the product after dimerisation, i.e. cracking and secondary dimerisation. It is clear from Figure 3-13 that the product ratio evens out quickly, irrespective of the reaction temperature or the residence time. Therefore, to correlate the product distribution with regard to the amount of dimerised hexene (D), the cracking distribution can be defined as specified by K_{eq} (Equation 3-1). The determined K_{eq} values can be represented by a Van't Hoff relationship, Figure 3-17. The straight-line relationship is not perfect over the entire temperature range, although the general trend obeys the Van't Hoff relationship.

It is clear that the formation of longer chain olefins (C_{12} and C_{13}) is favoured at low temperatures whereas the formation of cracked (and secondary dimerised) product is favoured at higher temperatures.

If the predicted temperature relationship is compared to the product distribution observed for the dimerisation of DMB (Figure 3-18), a large divergence in the resulting formation of cracked products is evident. There is a greater selectivity to the formation of secondary cracked products (C_8, C_9 and C_{10}) from the dimerisation of shorter chain olefins (C_4, C_5 and C_7), for DMB. DMB will form predominantly branched products in comparison to 1-hexene, especially at lower temperatures, as such more cracking will occur more readily to lower chain olefins which will then convert quickly due to the increased reaction rate of shorter chain olefins. By contrast, the formation of longer chain olefins (C_{11}, C_{12} and C_{13}) correlate well with the 1-hexene product spread, especially at higher temperatures. The differences seen in the product formation from DMB dimerisation and 1-hexene dimerisation can be linked to the lack of CD for the dimerisation of DMB. Since it is not possible to distinguish which products (carbon length) originate from CD or from the DBH, the comparison of the product distribution between 1-hexene and DMB is mute.

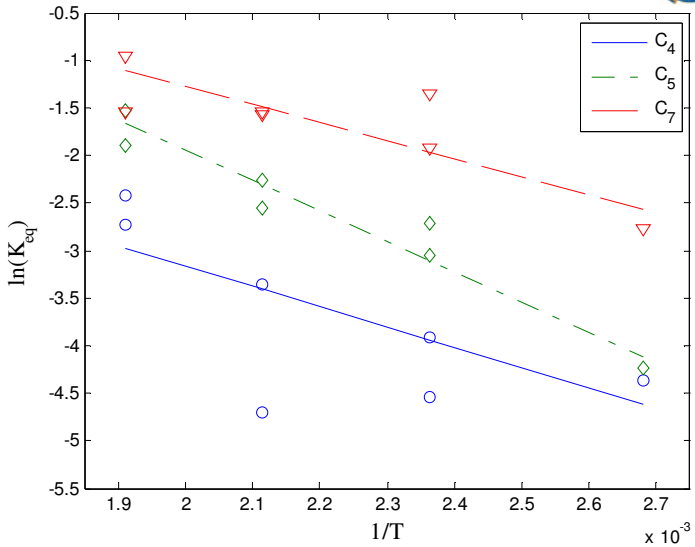

a) ○ - C_4, ◊ - C_5 and ▽ - C_7

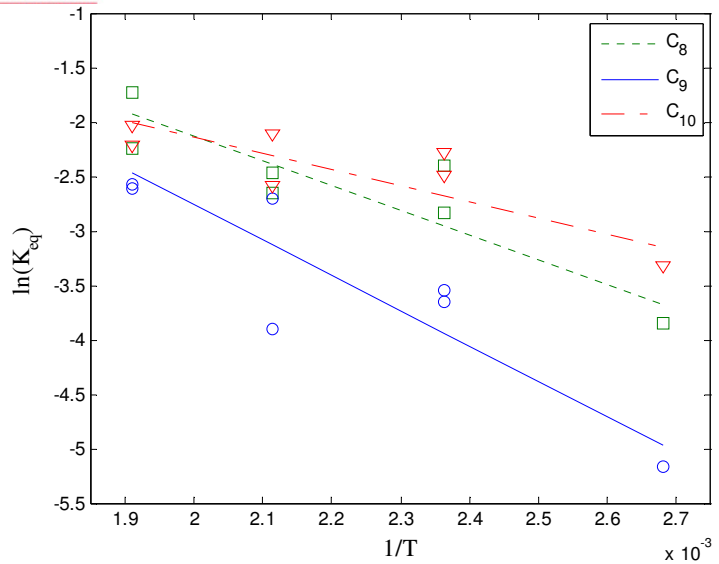

b) □ - C_8, ○ – C_9 and ▽ - C_{10}

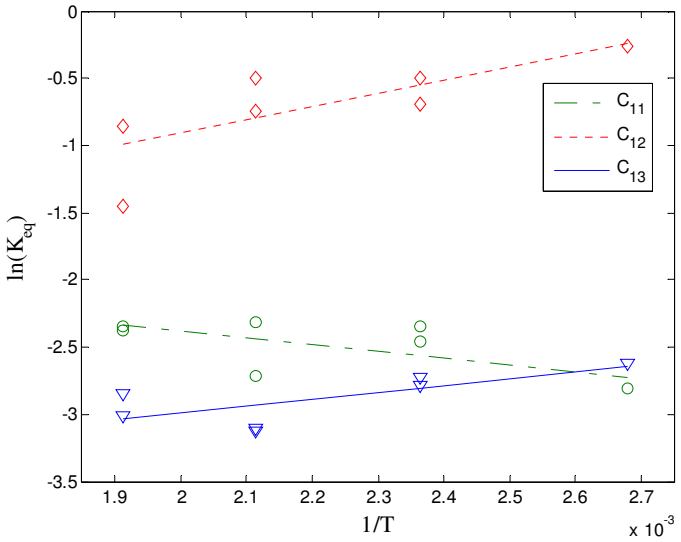

c) ○ - C_{11}, ◊ - C_{12} and ▽ - C_{13}

Figure 3-17: $\ln(K_{eq})$ for each carbon number versus 1/T for 1-hexene dimerisation (excluding C_6) *a)* C_4, C_5 and C_7, *b)* C_8, C_9 and C_{10} and *c)* C_{11}, C_{12} and C_{13}.

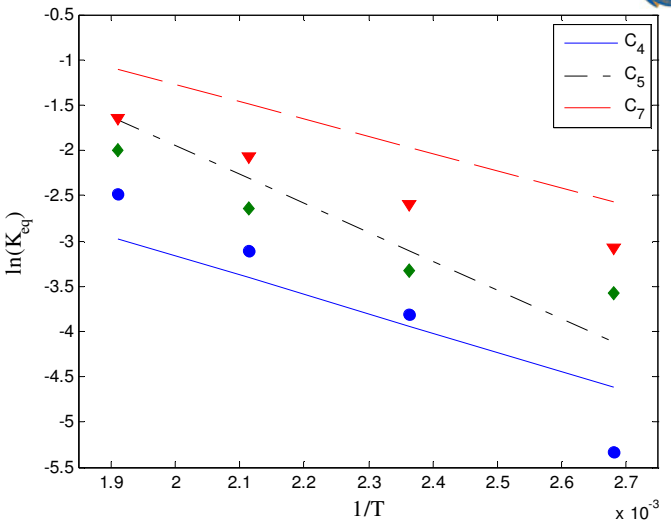

a) ○ - C_4, ◊ - C_5 and ▽- C_7

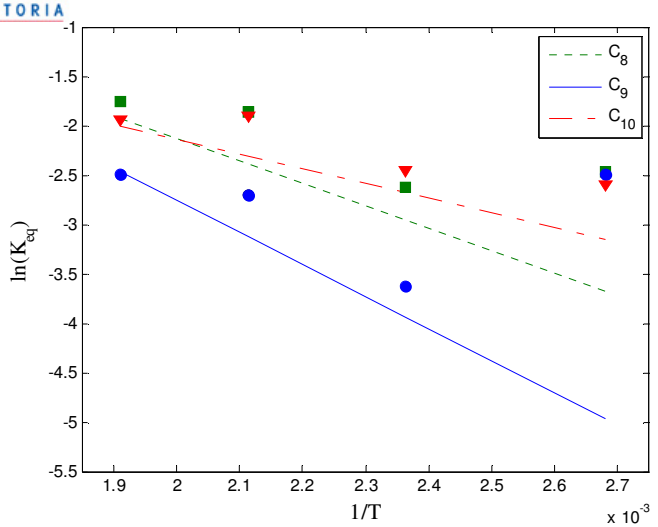

b) □ - C_8, ○ - C_9 and ▽- C_{10}

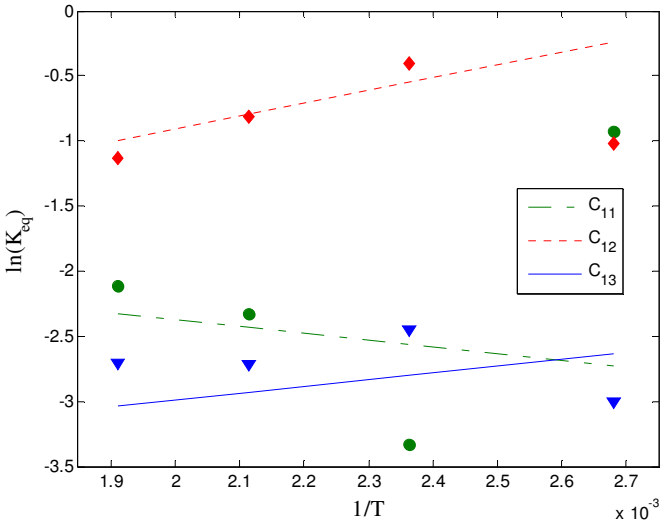

c) ○ - C_{11}, ◊ - C_{12} and ▽- C_{13}

Figure 3-18: $\ln(K_{eq})$ for each carbon number versus 1/T for DMB dimerisation a) C_4, C_5 and C_7, b) C_8, C_9 and C_{10}, and c) C_{11}, C_{12} and C_{13}, the solid lines representing the carbon distribution observed for 1-hexene dimerisation (Figure 3-17).

3.5 Conclusions

A reaction mechanism was proposed for the dimerisation of 1-hexene whereby dimerisation can occur by the dimerisation of linear hexenes (DLH) or, after skeletal isomerisation has occurred, by the co-dimerisation of linear and branched hexenes (CD) as well as the dimerisation of branched hexenes (DBH). To determine the kinetic parameters, kinetic experimental data was obtained, using a batch reactor from 100 – 250 °C for both 1-hexene and DMB as reagents.

The reaction rate was described, using a simple elementary kinetic model which resulted in a good description of the dimerisation of DMB and of 1-hexene. When modelling the reaction rate, it was found that the rate of DLH was negligible. Indicating that skeletal isomerisation needs to take place before oligomerisation of the hexenes will occur. Only the DBH and CD were needed to model the reaction rate, with CD taking place mainly at lower temperatures and DBH mainly at higher temperatures.

It was shown from the analysis of the reaction product that the carbon number distribution reached an equilibrium distribution almost instantaneously. Therefore the extent of cracking is solely a function of temperature. The resulting carbon number distribution from the cracking of dimerised product could be described, using a simple equilibrium distribution which resulted in an adequate prediction of the carbon number distribution for 1-hexene dimerisation.

The oligomerised product also contained high fractions of aromatics, even at lower temperatures, which increased with temperature. Aromatic formation has been shown to occur for propene oligomerisation by Ipatieff (1935) and Ipatieff and Corson (1936) although at much higher temperatures. Van der Westhuizen *et al.* (2010) showed the presence of aromatic precursors at lower temperatures, for light olefin oligomerisation. Therefore it is concluded that the aromatic formation is propagated with the addition of 1-hexene to the reaction mixture.